

X-ray Diffraction from Fatty-Acid Multilayers. Angular Width of Reflexions from Systems with Few Unit Cells

BY W. LESSLAUER

Institute for Pathology, University of Basel, Switzerland

(Received 6 December 1973; accepted 26 March 1974)

Fatty-acid multilayers are highly diffracting systems. The number of unit cells is known from the manner in which they are prepared. Systems with from two to ten unit cells were studied by X-ray diffraction. The angular width of reflexions was observed to be a function of the number of unit cells. It can be substantiated that under these conditions the sampling of the absolute square of the structure factor occurs by an interference function whose main maxima possess finite width around the reciprocal lattice points. The implications of these observations for a direct analysis of the intensity data are discussed.

Introduction

Multilayer systems of salts of long-chain fatty acids can be prepared by the technique of Blodgett (1935). They are built up on solid substrates by multiple passes through a monomolecular film of the fatty acid on the surface of an electrolyte solution. These multilayers are a sequence of stacked, parallel bilayers. They are highly diffracting systems. The number of bilayers, N , in the multilayer is equal to half the number of passes through the monolayer. Diffraction of X-rays can thus be recorded from systems with known numbers of unit cells. The case of multilayers with small N (*i.e.* $N=2-10$) is of interest both for methodological and for theoretical reasons. (1) The experimental test of whether sampled diffraction data can be recorded from membrane-like systems with but a few cells relates to the general suitability of low-angle diffraction in the study of the structure of biological membranes. Diffraction methods have proved useful for special membrane systems such as myelin or photoreceptor membranes (*e.g.* Worthington, 1971) where naturally N is large. These systems are exceptional, but systems with a few stacked membranes may be prepared more readily. (2) The sampling of the absolute square of the structure factor in the case of small N is by an interference function whose maxima possess finite width. It follows from the theories of Hosemann & Bagchi (1962) that under these conditions the intensity information in the diffraction pattern may suffice for a direct determination of the structure.

The electron density function $\varrho(z)$ of a multilayer system with small N (where z is a coordinate perpendicular to the bilayer planes) is conveniently described by a convolution of the density function of one bilayer $\varrho_0(z)$ with a finite lattice peak function

$$\varrho(z) = \varrho_0(z) * [s(z) \sum_{h=-\infty}^{\infty} \delta(z-hd)] \quad (1)$$

where $s(z)$ is the one-dimensional shape function [$s(z)=1$ for $|z| \leq Nd/2$, $s(z)=0$ for $|z| > Nd/2$ and $\int s(z)dz =$

Nd], d the cell dimension in the z direction and $\delta(z)$ a Dirac delta function. * stands for a convolution operation. The transform of $\varrho(z)$ is $T(Z)$. It becomes, with the convolution theorem,

$$T(Z) = \frac{1}{d} F(Z) [S(Z) * \sum_{h=-\infty}^{\infty} \delta(Z-h/d)] \quad (2)$$

where

$$\varrho_0(z) \Leftrightarrow F(Z) \quad s(z) \Leftrightarrow S(Z) = Nd \operatorname{sinc}(\pi NdZ)$$

and

$$\sum_h \delta(z-hd) \Leftrightarrow \frac{1}{d} \sum_h \delta(Z-h/d).$$

The symbol \Leftrightarrow stands for Fourier transformation. The diffracted intensities are proportional to the absolute square of the transform, $|T(Z)|^2$,

$$|T(Z)|^2 = \frac{1}{d^2} |F(Z)|^2 [|S(Z)|^2 * \sum_{h=-\infty}^{\infty} \delta(Z-h/d)] = |F(Z)|^2 J(N, Z). \quad (3)$$

The interference function $J(N, Z)$ is then represented by functions of the type $(Nd)^2 \operatorname{sinc}^2(\pi NdZ)$ placed at every reciprocal lattice point by the convolution with $\sum_h \delta(Z-h/d)$. For the following considerations it is assumed that the secondary maxima of the sinc^2 functions are small compared with the main maximum and that they may be neglected. If then the integral width β_a of a peak of the interference function as given in equation (3) is defined in a way analogous to that of von Laue (1926) as the ratio of the integral A of $J(N, Z)$ over the neighbourhood of a reciprocal lattice point,

$$A = \int_{h/d-\varepsilon}^{h/d+\varepsilon} J(N, Z) dZ \quad [\varepsilon = 1/(2d)]$$

to its maximum value $J(h/d)$, one obtains with the approximation

$$A \simeq \int_{h/d-\varepsilon}^{h/d+\varepsilon} |S(Z)|^2 dZ \simeq Nd$$

for the integral width $\beta_a \simeq 1/(Nd)$.

Since the experimentally observed quantity is the angular width of reflexions, it is more convenient to express this result as the integral angular width of a peak of $J(N, Z)$, β :

$$\beta = \lambda / (Nd \cos \theta) \quad (4)$$

where λ is the wavelength of the radiation and 2θ the diffraction angle. This result is a special case of the general expression for the integral width of Debye-Scherrer lines derived by Stokes & Wilson (1942).

A generalized form of the Patterson function, $P'(z)$, is obtained either from $P'(z) = \rho(z) * \rho(-z)$ or from equation (3) by $P'(z) \leftrightarrow |T(Z)|^2$,

$$P'(z) = \frac{1}{d} P_0(z) * [\sigma(z) \sum_{h=-\infty}^{\infty} \delta(z - hd)] \quad (5)$$

where $P_0(z)$ is the autocorrelation function, $P_0(z) = \rho_0(z) * \rho_0(-z)$. $P_0(z)$ has a width of $2d$. $\sigma(z)$ is a triangular function with $\sigma(z) = Nd[1 - |z|/(Nd)]$ for $|z| \leq Nd$ and $\sigma(z) = 0$ for $|z| > Nd$. Then $[\sigma(z) \sum \delta(z - hd)]$ is a scaled lattice peak function from $-Nd$ to $+Nd$, where the j th peak has a scaled value of $(N - |j|)d$. The generalized Patterson function, therefore, is non-periodic; it can be represented by the sum of scaled and overlapping autocorrelation functions $P_0(z)$ placed at jd ($-N \leq j \leq +N$). It is obvious that as $N \rightarrow \infty$, $P'(z)$ degenerates into the common Patterson function.

In the analysis of a structure $P'(z)$ has to be calculated from the intensity data, which are for the case of small N discussed here a continuous function of Z . This can be done by choosing an arbitrary sampling interval ΔZ for the intensity function. By introducing a fractional coordinate ζ such that $Z = \zeta \Delta Z$, $P'(z)$ becomes

$$P'(z) = \int_{-\infty}^{\infty} |T(Z)|^2 \exp(-2\pi izZ) dZ \\ \approx 2\Delta Z \sum_{\zeta} |T_{\zeta}|^2 \exp(-2\pi iz\zeta \Delta Z). \quad (6)$$

$P'(z)$ calculated by the approximation in equation (6) is strictly non-periodic only in the limit $\Delta Z \rightarrow 0$. For finite ΔZ , $P'(z)$ calculated in this way has a period of $1/\Delta Z$. Then ΔZ must be chosen in a manner to avoid overlapping from neighbouring $P'(z)$; this condition is met if $1/\Delta Z \gg 2Nd$. Obviously, the experimentally derived $P'(z)$ does not include contributions from $|T_{\zeta}|^2$ for ζ which are smaller than a certain minimum value ζ_{\min} , since diffraction cannot be recorded around the origin. Also, it is of limited resolution, corresponding to the reciprocal-space cut-off at a certain ζ_{\max} in the diffraction pattern. The experimental generalized Patterson function $P'_{\text{exp}}(z)$ thus uses only a part of the intensity function given by the product of $|T(Z)|^2$ with a window function $W(Z)$ of width $\Delta\zeta = \zeta_{\max} - \zeta_{\min}$ and centred at $|Z| = \Delta\zeta/2$. It follows that $P'_{\text{exp}}(z) = P'(z) * [w(z) 2 \cos(\pi \Delta\zeta z)]$, where $w(z) = \Delta\zeta \text{sinc}(\pi \Delta\zeta z)$.

Materials and methods

Details on the preparation of the fatty-acid multilayers according to Blodgett (1935) are given in the preceding article. For a multilayer with small N special care has to be taken that a whole number of bilayers is transferred into the multilayer system. This can be done by removing the monomolecular film from the water surface before the support is finally withdrawn. Also, the monomolecular film must be spread and handled with special care in order to make certain that a true monolayer is transferred in every pass. Details of the procedure for building up multilayers with the desired structure must be determined by trial and error. Even then an occasional specimen may show minor diffraction phenomena superimposed on the typical lamellar diffraction.

Details of diffraction experiments are given in the preceding article. Diffraction patterns were recorded on Ilford Industrial G X-ray film. Densitometer traces of diffraction patterns were obtained with a Joyce-Loebl double-beam microdensitometer MK IIIb with an effective slit width of $15 \mu\text{m}$ or less. The effective slit width, therefore, was always less than 0.4% of the spacing of the lamellar reflexions in the diffraction patterns.

Results and analysis

X-ray diffraction was recorded from barium stearate multilayers with $N=2, 3, 4, 5, 6$ and 10 and from magnesium stearate multilayers at 100% relative humidity with $N=2, 3$ and 31 (Fig. 1). It appears from Fig. 1, and can be verified from densitometer traces of the patterns reproduced in Fig. 2 that with the barium stearate structures the peak maxima occur in regular intervals proportional to $1/46.9 \text{ \AA}^{-1}$. The standard variations for the positions of the peak maxima for the different N are the equivalent of about ± 0.5 – 1.0 \AA and no significant asymmetries of the peaks with respect to the reciprocal lattice points $h/46.9 \text{ \AA}^{-1}$ are observed. It may be concluded, therefore, that within the limits of the experimental errors the positions of the peak maxima of the intensity functions coincide with those of the peak maxima of the interference function at h/d . The spacings h/d do not significantly depend on N .

Only a few reflexions were observed with the magnesium stearate structures with small N . The variations in the spacings of the reflexions were larger than with barium stearate and, in particular, the fifth and sixth reflexions are shifted by a larger amount than expected from the variations of the spacings in the barium stearate structures (the spacing of the peak maxima of reflexions 4 and 5 is $1.07/d$ and that of reflexions 5 and 6 is $0.89/d$). Although reflexions 5 and 6 are weak, these shifts may be significant and due to the fact that the sampling here occurs in a region where $d[|F(Z)|^2]/dZ$ is large.

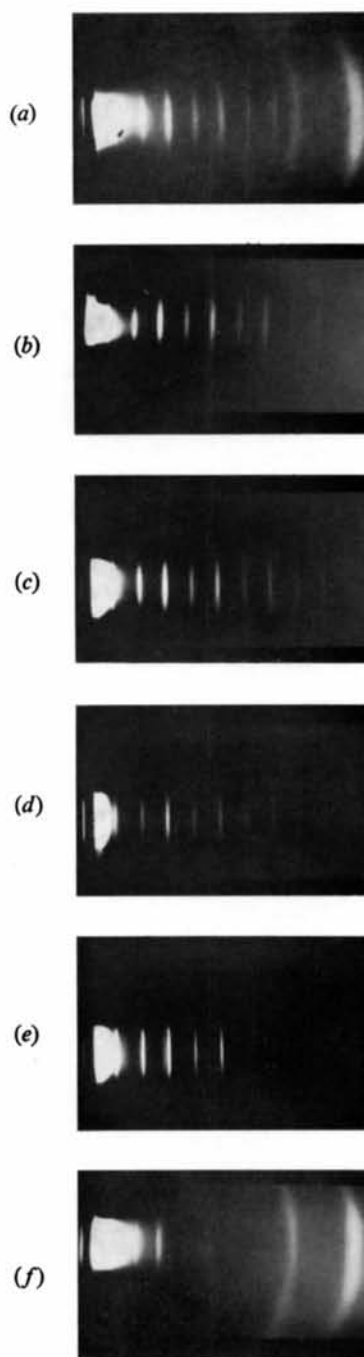


Fig. 1. Examples of diffraction patterns from barium stearate multilayers with 2 (*a*), 3 (*b*), 4 (*c*), 5 (*d*) and 10 (*e*) bilayers and from magnesium stearate multilayers at 100% relative humidity with 3 (*f*) bilayers. Films of approximately equal density were chosen. (Contact prints of the original diffraction patterns. The added weak scattering in (*a*) originates from the camera set-up in that experiment.)

The angular width of the reflexions does very clearly vary inversely with N (Figs. 1, 2). A quantitative evaluation of this variation is given in Figs. 3 and 4. Fig. 3 presents normalized densitometer traces of the third reflexions of the barium stearate multilayers with different N . The third reflexions were chosen, because

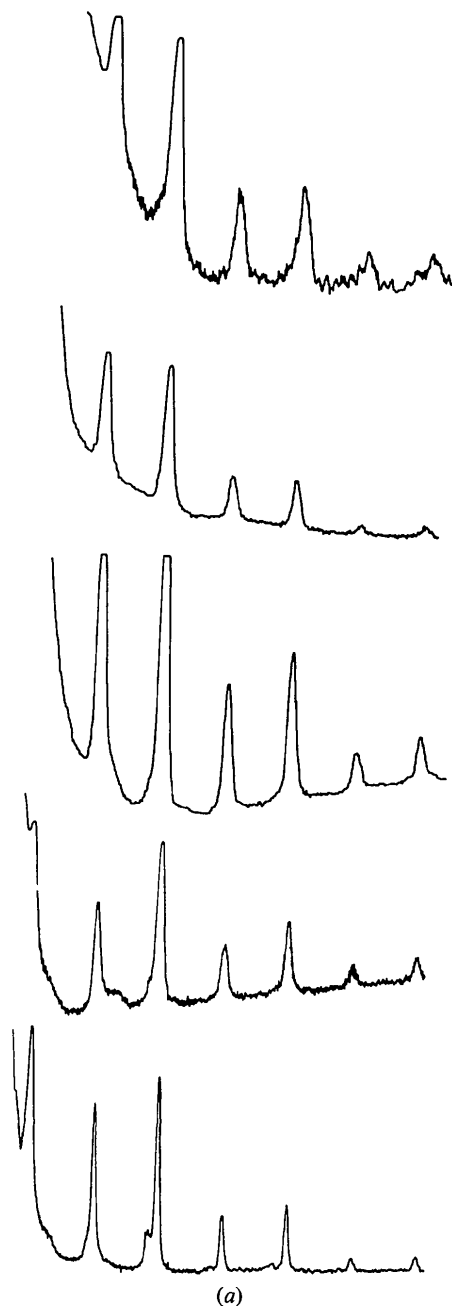


Fig. 2. (a) Densitometer traces of diffraction patterns from barium stearate multilayers with (from top to bottom) 2, 3, 4, 5 and 10 bilayers. The examples given were chosen because they had comparable densities and could be densitometered with the same optical wedge and slit settings ($h=1-7$).

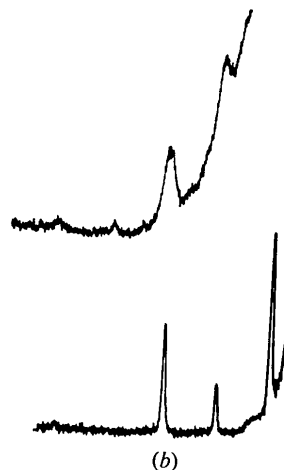


Fig. 2 (cont.) (b) Densitometer tracings of diffraction patterns from magnesium stearate multilayers at 100% relative humidity with 3 (top) and 31 (bottom) bilayers ($h=-1, -2, -3$).

they are strong and the level of background radiation on either side of the reflexions is approximately the same. Also, corrections for oblique incidence of the diffracted ray on the film may be neglected. The measured integral angular width β as a function of N is given in Fig. 4 together with the theoretical values. In Fig. 4, β has been corrected for (a) camera geometry and (b) the fact that $|F|^2$ for the barium stearate bilayer is not constant in the sampling interval $2/(Nd)$ centred at h/d . The error resulting if the integral width of the reflexion β_i is taken for β becomes obvious from the following considerations for the case $N=2$. The bilayer structure can be represented by the model (see preceding paper)

$$\rho(z) - \bar{\rho} \approx P \cdot g_p(z) * [\delta(z - d/2) + \delta(z + d/2)] - M \cdot g_m(z) * \delta(z)$$

where $g_{p,m}(z)$ are normalized Gaussian functions and P and M scaling factors. The Gaussians can be assumed to be narrow. Furthermore, the scaling factor P is larger than M . Then $|F|^2$ for the model structure is of the type $4P \cos^2(\pi dZ)$ in the range of Z considered in this discussion. The interference function for $N=2$ is $4 \cos^2(\pi dZ)$. The integral width of peaks of the interference function and of the intensity function, β and β_i , for this model can be calculated analytically, and their ratio becomes $\beta/\beta_i = 4/3$. The integral width of peaks of the intensity function, which is the experimentally observable quantity, must then be corrected in order to obtain β . The correction factors β/β_i which were applied to the experimental data in Fig. 4 were derived from an analogous comparison of the intensity and interference functions. The interference function was computed from

$$J(N, Z) = N + 2 \sum_{n=1}^{N-1} (N-n) \cos(2\pi n d Z)$$

and $|F(Z)|^2$ was reconstructed after the Fourier sampling theorem (Shannon, 1949; Sayre, 1952) with data from barium stearate multilayers with many unit cells (see preceding article). The intensity function is then given by equation (3). It is noted that β_i is independent of the absolute value of $|F(h/d)|^2$, and the correction factors are readily obtained from the thus computed intensity and interference functions. For the barium stearate data the values obtained are 1.30, 1.16 and 1.04 for $N=2, 3$ and 4. For $N > 4$, β/β_i is approximately 1.0. Similar arguments led to the calculation of the

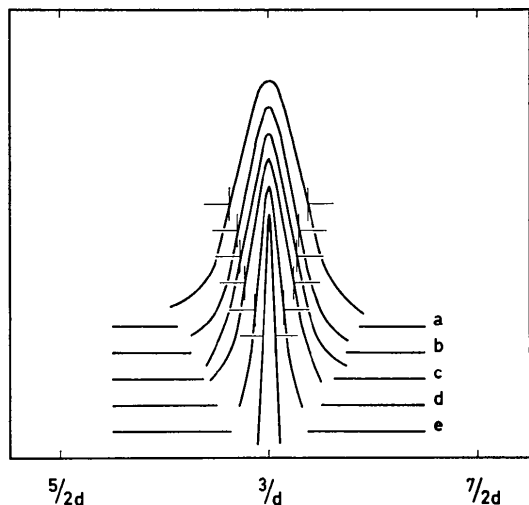


Fig. 3. Superposed densitometer traces of the third reflexions from barium stearate multilayers with 2 (a), 3 (b), 4 (c), 5 (d) and 10 (e) unit cells. The peaks are normalized to the same height at h/d . The respective base lines are marked a, b, c, d and e. The profile of the primary beam used in the experiments is included (innermost curve).

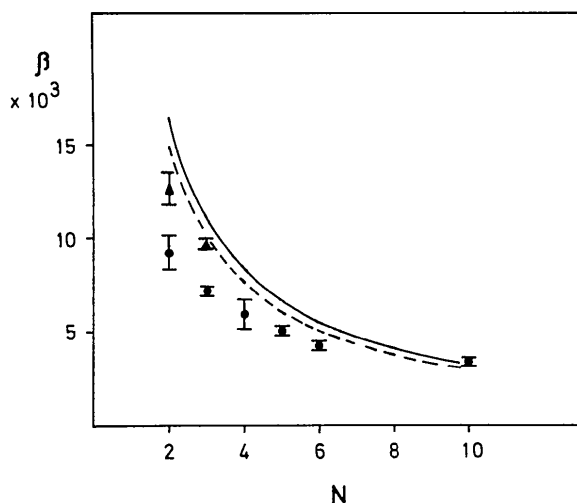


Fig. 4. Integral angular width β (with standard variation) as a function of the number of cells, N , in barium stearate (●) and magnesium stearate (▲) multilayers. The theoretical curves are included (the dashed curve refers to the magnesium stearate structure). β is given in radians.

correction factors for the width of the third reflexions of the hydrated magnesium stearate structures in Fig. 4.

Discussion

Theoretical and experimental values for β in Fig. 4 do not match exactly. It is obvious that for the smaller N especially the observed integral width is too small, although a significant increase in width with decreasing N is documented. Besides the mentioned correction factors, β/β_i , several additional factors have an influence on the measured width of reflexions.

(1) The primary beam is not monochromatic, parallel and homogeneous. Ni-filtered Cu $K\alpha$ radiation was used. The increase in β_i due to the non-monochromaticity may be neglected. If the difference in wavelength of Cu $K\alpha_1$ and Cu $K\alpha_2$ is taken as a measure of non-monochromaticity, the relative increase in width due to this factor is less than 0.01. No exact data on the homogeneity of the beam are available. However, the profile of the primary beam recorded under the same conditions as the patterns in Fig. 1 is a measure of its angular divergence. From this the influence of the beam profile can be evaluated. Both the primary beam (G_1) and the ideal diffracted beam without instrumental broadening (G_2) will be approximated by normalized and scaled Gaussian functions,

$$G_{1,2}(Z) = \alpha_{1,2} a_{1,2} \exp(-\pi a_{1,2}^2 Z^2)$$

with the integral widths of $1/a_1$ and $1/a_2$. The integral width of the reflexion which is observed under the given experimental conditions is then represented by the convolution $G_1 * G_2$ (Stokes, 1948). Using the faltings theorem this can easily be shown to be another Gaussian function of an integral width of $(1/a_1^2 + 1/a_2^2)^{1/2}$. If the ratio of the measured widths of the reflexions to the width of the primary beam is called τ , the relative error due to beam divergence becomes $\sim 1/(2\tau^2)$. From Fig. 3, τ can be estimated. It follows then that the relative error in β_i caused by beam divergence increases from 0.01 for $N=2$ to 0.10 for $N=10$. If the measured values in Fig. 4 were corrected for this broadening, they would fall on a curve roughly parallel to the theoretical curve. The measured values are, however, systematically too small by an average of about 25% of the measured value.

(2) The diffuse radiation background of the camera and the characteristics of the X-ray film contribute to the experimental errors in β . On the densitometer traces a linear interpolation of the minima on either side of the lamellar reflexions was taken as base line. Both parasitic scattering from slits, windows and beam stop and incoherently scattered radiation add to this base line, which has in typical patterns a density of about 0.5–1.0 O.D. Microdensitometer traces were recorded with an optical wedge with a range of 3.0 O.D. Peak maxima were typically about 2.0 O.D. above base line. The relation between exposure and density of photographic emulsions for X-rays is linear for low

exposures. At higher exposures resulting in densities larger than about 1.0 this linear relation is no longer valid. The photographic film used in these experiments deviates significantly from the proportionality of exposure and density above about 1.5 O.D. (Commission on Crystallographic Apparatus, 1956). The densities at the peak maxima, therefore, are no longer in the linear range of the emulsion. The observed densities on the film then are the same as those which were observed with an ideally linear emulsion in a hypothetical camera designed in such a way that the background radiation exclusively fills up the minima around the reflexions. Therefore, the base line chosen on the densitometer traces of the diffraction patterns by the above-mentioned criterion is too high by an undetermined amount, and the measured width of the reflexions is proportionately too small. It should be noted also that for small N larger than $N=2$ there are secondary diffraction peaks in the region between the main lamellar reflexions at about h/d which can be observed occasionally. The existence of these secondary diffraction maxima increases the difficulties in finding the true minima on either side of the main lamellar reflexions.

(3) With regard to the microdensitometer, an optimum between resolution and sensitivity obviously has to be found for the slit settings of the optical system of the instrument.

Despite these limitations it is obvious that the observed broadening of reflexions for decreasing N is due to the fact that $|F|^2$ is sampled by an interference function with peaks of finite width around h/d . The continuous intensity curve from these patterns, therefore, provides information not only on the value of the absolute square of the structure factor at the ideal reciprocal lattice point h/d , but also in its neighbourhood. The gain in information compared with diffraction data from systems with large N is similar to that in swelling experiments, where the same transform is sampled in slightly different intervals.* A convenient analysis of these data is by the generalized Patterson function $P'(z)$, which can be used to obtain the autocorrelation function $P_0(z)$, and consequently the electron density function $\rho_0(z)$ by a deconvolution of $P_0(z)$

* To show the equivalence of swelling experiments and the present arguments assume that continuous $|F(Z)|^2$ is known [$\rho_0(z) = \rho_0(-z)$]. Then $\rho_0(z)$ can be calculated, because the continuous $|F(Z)|^2$ fixes the phase signs, or alternatively, because the transform of $|F(Z)|^2$ yields the autocorrelation function $P_0(z)$, which can be deconvoluted. In swelling experiments $|F(Z)|^2$ is sampled in intervals h/d corresponding to the normal period d and in addition in slightly different intervals $1/d_1, 1/d_2$, etc. with swollen structures such that $|F(Z)|^2$ becomes known in a certain region around each h/d . What is known then is the product of $|F(Z)|^2$ with a series of window functions $W(Z)$ placed at each h/d . If this product is called $|F_{sc}|^2$, one can write

$$|F_{sc}(Z)|^2 = |F(Z)|^2 [W(Z) * \frac{1}{d} \sum_h \delta(Z - h/d)].$$

A kind of Patterson function $P_{sc}(z)$ can be calculated in analogy with equation (6) by $|F_{sc}|^2 \Leftrightarrow P_{sc}$,

(Hosemann & Bagchi, 1962). The main effects of experimental errors in the recorded intensities on $P'(z)$ can be discussed in relation to equations (3) and (5). The relative error in the experimentally determined width β_i with respect to the theoretical value $\beta_{i, \text{theor}}$ will be called γ , i.e. $\gamma = (\beta_i - \beta_{i, \text{theor}}) / \beta_{i, \text{theor}}$. This is most conveniently expressed as an error in the integral width of the term $|S(Z)|^2$ in equation (3). From equation (5) it follows then that $P'(z)$ will be terminated by the term $\sigma(z)$ at $|z| = (1 - \gamma) / \beta_{\text{theor}}$. Therefore, $P'(z)$ will not disappear exactly at $|z| = Nd$, but rather will extend to higher values of $|z|$ to an amount determined by γ . Consequently the scaling down of $P'(z)$ will be too slow and its values at the lattice points $z = jd$ will be $P'(jd) = d[N - |j| / (1 - \gamma)] P_0(0)$ ($-N \leq j \leq N$). It could be demonstrated, however, that the direct analysis of the recorded intensity function by a deconvolution of $P_0(z)$ can be performed successfully with the data from the stearate multilayers despite these experimental errors (Lesslauer, 1971; Lesslauer & Blasie, 1972).

Conclusions

From the general properties of the fatty-acid multilayers (e.g. Bücher *et al.*, 1967) there is little doubt that under appropriate experimental conditions one single monolayer is incorporated into the multilayer every time it passes through the monomolecular film on the water surface. Therefore, the number of bilayers in the system is known exactly. Discrete reflexions can be recorded in X-ray diffraction experiments with such systems containing as few as two unit cells. It can be substantiated that the increase in width of reflexions observed with decreasing N is due to the fact that $|F(Z)|^2$ is sampled over observable finite intervals around the reciprocal lattice points. The demonstration of this result is relevant, because a direct analysis of diffraction data becomes feasible under these conditions.

Diffraction experiments were performed during the author's stay at the Department of Biophysics and Physical Biochemistry of the University of Pennsyl-

$$P_{sc}(z) \sim \text{const} \cdot \Delta Z \sum_{\zeta} |F_{sc}(\zeta)|^2 \exp(-2\pi i z \zeta \Delta Z).$$

From the definition of $|F_{sc}|^2$ and the faltung theorem it follows that P_{sc} can be represented by

$$P_{sc}(z) = P_0(z) * [w(z) \sum_h \delta(z - hd)].$$

P_{sc} is then the sum of autocorrelation functions placed at h/d by the scaled lattice peak function $[w(z) \sum_h \delta(z - hd)]$, where $P_{sc}(hd) = P_0(0)w(hd)$. Since $w(z)$ is a known function [i.e. of the type $\text{sinc}(z)$], the autocorrelation function can be obtained from P_{sc} . Once $P_0(z)$ is known, the electron-density function is also known, because the continuous $|F(Z)|^2$ can be calculated by $P_0(z) \Leftrightarrow |F(Z)|^2$ and the phase signs of reflexions, therefore, are determined, or alternatively, because $P_0(z)$ can be deconvoluted. Throughout this discussion the assumption is made that the correct solution among the symmetry-related solutions can be recognised by independent reasoning.

vania, Philadelphia. During that time he was supported by funds from the Johnson Research Foundation. Computations were done on a PDP 9 (Inst. Phys. Chem., University of Basel). The microdensitometer was on loan from CIBA-Geigy AG (Basel). The work was supported in part by the Schweizer Nationalfonds (3.8850.72).

References

- BLODGETT, K. B. (1935). *J. Amer. Chem. Soc.* **57**, 1007–1022.
 BÜCHER, H., DREXHAGE, K. H., FLECK, M., KUHN, H., MÖBIUS, D., SCHÄFER, F. P., SONDERMANN, J., SPERLING, W., TILLMANN, P. & WIEGAND, J. (1967). *Mol. Cryst.* **2**, 199–230.
 COMMISSION ON CRYSTALLOGRAPHIC APPARATUS (1956). *Acta Cryst.* **9**, 520–525.
 HOSEMANN, R. & BAGCHI, S. N. (1962). *Direct Analysis of Diffraction by Matter*, pp. 120–131, 514–524. Amsterdam: North Holland.
 LAUE, M. VON (1926). *Z. Kristallogr.* **64**, 115–142.
 LESSLAUER, W. (1971). *Proc. I. Eur. Biophys. Congress, Baden/Vienna*, Vol. IV, pp. 425–429.
 LESSLAUER, W. & BLASIE, J. K. (1972). *Biophys. J.* **12**, 175–190.
 SAYRE, D. (1952). *Acta Cryst.* **5**, 843.
 SHANNON, C. E. (1949). *Proc. Inst. Radio Engrs. N.Y.* **37**, 10–21.
 STOKES, A. R. (1948). *Proc. Phys. Soc.* **61**, 382–391.
 STOKES, A. R. & WILSON, A. J. C. (1942). *Proc. Camb. Phil. Soc.* **38**, 313–322.
 WORTHINGTON, C. R. (1971). In *Biophysics and Physiology of Excitable Membranes*, edited by W. J. ADELMAN, pp. 1–46. New York: Van Nostrand.

Acta Cryst. (1974). B30, 1937

Hydrogen Bond Studies. LXXXVI.* An Asymmetric Non-Centred H_5O_2^+ Ion: Neutron Diffraction Study of Picrylsulphonic Acid Tetrahydrate, $[\text{H}_5\text{O}_2]^+[\text{C}_6\text{H}_2(\text{NO}_2)_3\text{SO}_3]^- \cdot 2\text{H}_2\text{O}$

BY JAN-OLOF LUNDGREN AND ROLAND TELLGREN

Institute of Chemistry, University of Uppsala, Box 531, S-751 21 Uppsala, Sweden

(Received 1 March 1974; accepted 16 April 1974)

A three-dimensional single-crystal neutron diffraction study has been made of picrylsulphonic acid tetrahydrate. The crystals are triclinic, space group $P\bar{1}$, with two formula units in a cell of dimensions: $a=8.346$ (1), $b=11.367$ (1), $c=8.065$ (2) Å, $\alpha=97.77$ (2), $\beta=109.32$ (1), $\gamma=83.22$ (1)°. A full-matrix least-squares refinement based on F^2 gave a final R value of 0.052. The structure comprises H_5O_2^+ ions, picrylsulphonate ions and water molecules. The diaquahydrogen ion is of the asymmetric non-centred type. The hydrogen atom in the short [2.436(2) Å] practically linear hydrogen bond is situated 0.09 Å from the centre of the bond. X-ray – neutron (X–N) difference Fourier syntheses have been calculated to illustrate the asphericity of the atomic charge distribution in the H_5O_2^+ and picrylsulphonate ions.

Introduction

The diaquahydrogen ion, H_5O_2^+ , has been found in X-ray structure determinations of several hydrates of strong acids. However, no definite information as to the location of the hydrogen atoms of the H_5O_2^+ ion can be obtained from the X-ray studies. The configuration of the ion has thus been deduced from the positions of the non-hydrogen atoms. A neutron diffraction study of picrylsulphonic acid tetrahydrate was therefore undertaken to study the geometry of the diaquahydrogen ion in more detail. In this compound the hydrogen atom in the very short $\text{O} \cdots \text{O}$ bond has an asymmetric environment and is not forced by symmetry to be located in the centre of the bond. The X-ray structure determination of picrylsulphonic acid

tetrahydrate has been reported earlier by Lundgren (1972). This work is part of a series of systematic studies of solid hydrates of strong acids currently in progress at this Institute.

Crystal data

2,4,6-Trinitrobenzenesulphonic acid tetrahydrate (picrylsulphonic acid tetrahydrate), $\text{C}_6\text{H}_2(\text{NO}_2)_3\text{SO}_3\text{H} \cdot 4\text{H}_2\text{O}$. F.W. 365.23. Triclinic, $a=8.346$ (1), $b=11.367$ (1), $c=8.065$ (2) Å, $\alpha=97.77$ (2), $\beta=109.32$ (1), $\gamma=83.22$ (1)°, $V=713.2$ Å³ at 22°C. $Z=2$, $D_x=1.701$ g cm⁻³. Space group $P\bar{1}$ (Lundgren, 1972).

† Numbers in parentheses here and throughout this paper are the estimated standard deviations in the least significant digits.

* Part LXXXV: *J. Chem. Phys.* In the press.